Accepted Manuscript

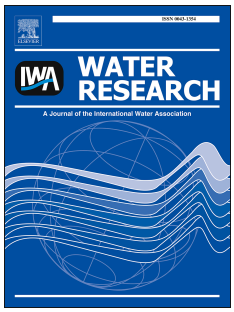

Immobilization of Cd in river sediments by sodium alginate modified nanoscale zero-valent iron: Impact on enzyme activities and microbial community diversity

Danlian Huang, Wenjing Xue, Guangming Zeng, Jia Wan, Guomin Chen, Chao Huang, Chen Zhang, Min Cheng, Piao Xu

PII: S0043-1354(16)30727-8

DOI: 10.1016/j.watres.2016.09.050

Reference: WR 12389

To appear in: *Water Research*

Received Date: 23 May 2016

Revised Date: 21 September 2016

Accepted Date: 24 September 2016

Please cite this article as: Huang, D., Xue, W., Zeng, G., Wan, J., Chen, G., Huang, C., Zhang, C., Cheng, M., Xu, P., Immobilization of Cd in river sediments by sodium alginate modified nanoscale zero-valent iron: Impact on enzyme activities and microbial community diversity, *Water Research* (2016), doi: 10.1016/j.watres.2016.09.050.

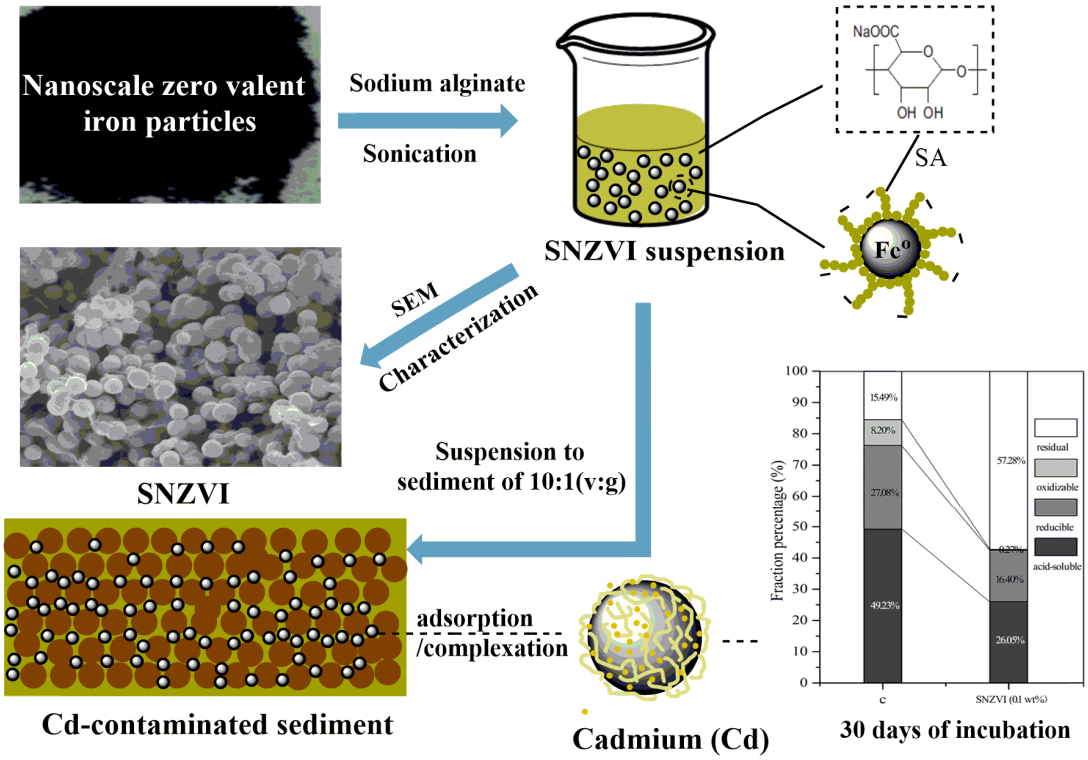

Immobilization of Cd in river sediments by sodium alginate modified nanoscale zero-valent iron: Impact on enzyme activities and microbial community diversity

Danlian Huang [a,b,*], *Wenjing Xue* [a,b], *Guangming Zeng* [a,b,**], *Jia Wan* [a,b], *Guomin Chen* [a,b], *Chao Huang* [a,b], *Chen Zhang* [a,b], *Min Cheng* [a,b], *Piao Xu* [a,b]

[a] College of Environmental Science and Engineering, Hunan University, Changsha, 410082, PR China

[b] Key Laboratory of Environmental Biology and Pollution Control (Hunan University), Ministry of Education, Hunan University, Changsha, 410082, PR China

Abstract

This paper investigated how sodium alginate (SA)-modified nanoscale zero-valent iron (NZVI), play a constructive role in the remediation of cadmium (Cd) contaminated river sediments. The changes of the fraction of Cd, enzyme activities (urease, catalase, dehydrogenase) and bacterial community structures with the treatment by SNZVI were observed. The sequential extraction experiments demonstrated that most mobile fractions of Cd were transformed into residues (the

* Corresponding author. College of Environmental Science and Engineering, Hunan University, Changsha, 410082, PR China.

** Corresponding author. College of Environmental Science and Engineering, Hunan University, Changsha, 410082, PR China.

E-mail address: huangdanlian@hnu.edu.cn (D. Huang), zgming@hnu.edu.cn (G. Zeng).

maximum residual percentage of Cd increases from 15.49% to 57.28% after 30 days of incubation at 0.1 wt% SA), with the decrease of bioavailability of Cd. Exclusive of dehydrogenase, the activities of the other two enzymes tested were enhanced with the increase of incubation time, which indicated that dehydrogenase might be inhibited by ferric ions formed from SNZVI whereas no obvious inhibition was found for other enzymes. Polymerase chain reaction denaturing gradient gel electrophoresis (PCR-DGGE) analyses were used for the detection of microbial community changes, and the results showed that SNZVI and NZVI could increase bacterial taxa and improve bacterial abundance. All the experimental findings of this study provide new insights into the potential consequences of SNZVI treatments on the metal Cd immobilization in contaminated river sediments.

Keywords

Nanoscale zero-valent iron; Sodium alginate; Cd; Enzyme activities; PCR-DGGE

1. Introduction

River sediments are basic components of our environment (Akcay et al., 2003). Recently, the sediment with heavy metal pollution has attracted more and more widespread attention due to its high toxicity, and even at a low concentration it can cause a great harm to living organisms (De Jonge et al., 2012; Olivares-Rieumont et al., 2005; Zhang et al., 2016a). Cadmium (Cd) is one of the major environmental pollutants in China and other countries/regions of the earth (Fassett et al., 1975; Huang et al., 2015). Pollution of sediments with Cd causes its incorporation into the food chain, which could result in a wide variety of adverse effects in animals and

humans, especially because it is a cumulative contaminant (Vinodhini et al., 2008). Consequently there is an imperative need to remediate Cd-contaminated sediments.

Recent researches show that nanoscale zerovalent iron (NZVI) is promising in removing contaminants including heavy metals, the treatments of which make the heavy metals immobile and prevent their entering into the deeper sediment layers, rivers, and groundwater (Zhang et al., 2016b; Dror et al., 2012; Xu et al., 2012; Feng et al., 2010). NZVI is composed of a Fe (0) core and an iron oxide shell. The core acts as an electron donor source, promoting reduction of compounds and the shell enables sorption, surface complexation and electron transport from and to the core (Calderon and Fullana, 2015). And it has been proposed as an efficient material for Cd immobilization (Calderon and Fullana, 2015; Su et al., 2014). But due to the small particle sizes and large specific surface areas of NZVI, it is probable that NZVI is easy to aggregate (Cumbal et al., 2003). Maintaining a stable small particle diameter is important to achieve sufficient mobility to reach the target contaminants (Su et al., 2015; Kharisov et al., 2012). To avoid an agglomeration of the particles, surface stabilizers (e.g., polyelectrolyte, surfactant, biopolymer) can be used that have some special performance with electrostatic repulsion or steric stabilization (Dong and Lo, 2013; Sirk et al., 2009). They can be coated onto the surface of the NZVI to decrease agglomeration and enhance the mobility of NZVI (Kim et al., 2009). As one of surface stabilizers, sodium alginate (SA) is a linear copolymer and natural anionic macromolecules found in the cell walls of brown algae, and each monomeric unit of sodium alginate contains one carboxylate and two hydroxyl groups. Its general

structure is comprised of 1,4- linked-α-L-guluronic acid (G) and β-d-mannuronic acid (M) in alternating blocks of GG, MM and MG arranged in an irregular pattern (Borba et al., 2016; Zia et al., 2015). This chemical conformation is good for chemical reactions and linkages in view of the presence of reactive sites, such as hydroxyl and carbonyl groups along the backbone (Zia et al., 2015). Researchers have reported that sodium alginate (SA) can effectively eliminate heavy metal ions, such as Pb^{2+}, Cu^{2+}, and Cd^{2+} (Gong et al., 2016), which hence could be a promising polymeric material to coat NZVI for immobilizing metal ions in contaminated sediments. The molecular structures of sodium alginate (SA) and the schematic diagram of SA modified NZVI is shown in (Fig. 1).

A successful immobilization remediation technique must maintain reasonable low solubility and bioavailability of heavy metals (Ruttens et al., 2010). However, it is not completely achievable to judge and measure their toxicity, mobility and bioavailability on the basis of the total concentrations of the metals (Jain, 2004; Prica et al., 2010), and moreover detecting the metals speciations is indispensable, which is channelled back into remediation of river sediments. Enzymatic activities and microbial communities can directly address biological availability and toxicity of heavy metals, and help define the acceptable cleanup standards (Kumpiene et al., 2006). Enzyme activities are credible designators for the process of biological conversion in the river sediment (Zhou et al., 2005). Polymerase chain reaction-denaturing gradient gel electrophoresis (PCR-DGGE) as a powerful molecular method for rapid detection of microbial community changes or comparative

analysis of environmental samples offers more accurate information about distribution and composition of microbial species (Aydin et al., 2015).

Nanomaterials applied to contaminated river sediments can induce an important change in the mobility and bioavailability of the heavy metal with potential consequences on ecosystem health (Zou et al., 2016). In this study, sodium alginate (SA)-modified nanoscale zero-valent iron (NZVI) was synthesized and the performance of SNZVI in the remediation of Cd contaminated river sediments was investigated. The mobility and bioavailability of sediment Cd was investigated using the optimized European Community Bureau of Reference (BCR) three-step sequential extraction procedure. Sediment enzymatic activities and microbial community diversity were also studied to assess the effectiveness of Cd immobilization remediation using SNZVI.

2. Materials and methods

2.1. Sediment characteristics

Sediments were sampled from the Xiangjiang River, one of the tributaries of the Yangtze River in Hunan province in southern China. It drains an area of approximately 94,600 km^2 and has a total length of approximately 856 km (Zhang et al., 1989). In Hunan Province, there are abundant reserves of non-ferrous metals, and most of the ores used for mining, mineral processing and smelting of non-ferrous and rare metals are found in the middle and lower reaches of the Xiangjiang River; and the effluents from these intensive mining and industrial activities are discharged into the river (Zhang et al., 2009). With the development of industrial production and

105 enlargement of the cities, the lower reaches of the Xiangjiang River have been
106 polluted seriously day by day in recent years (Zeng et al., 2006). For the present study
107 contaminated sediments (0-20 cm depth) were collected from Changsha, which is
108 located in the lower Xiangjiang River. Samples were air dried, crushed and sieved (75
109 μm) and stored at 4 °C prior to the experiments.

110 The concentrations of metals in the sediment were determined after nitric acid
111 digestion employing US EPA standard method (EPA3050B, 1996). Atomic absorption
112 spectrophotometer (AAS, Agilent 3510, USA) was used to detect the concentrations
113 of metals in the samples. Potential ecological risk (PER) index developed based on
114 sedimentary theory was introduced to assess the ecological risk degree of heavy
115 metals in the present sediment. Risk index (RI) can be calculated by the formulas
116 proposed by Hakanson (Hakanson, 1980). Details about the procedures here used are
117 given in the Supplementary Materials. According to the PEI index, the potential risk
118 of the metals was 38 (Pb), 17 (Cu), 7 (Cr) and 1900 (Cd), showing the individual risk
119 of being low, low, low, and very high. The excess Cd results in an overall considerable
120 risk of the sediment (Supplementary Materials, Table S1). It shows that Cd
121 contributes the most to the potential environmental risk at the study region. In
122 addition, the fractionation pattern of the metals in the sediment samples, are given in
123 Fig. S1 (Supplementary Materials). Whereas the most Cd in the sediment was found
124 in the acid-soluble fraction (49.23%) (Fig. S1), indicating its higher mobility and
125 bioavailability compared to the other three metals (Peng et al., 2009). Thus, Cd was
126 selected as the main object of this study. The physical and chemical characteristics of

tested sediment were analyzed according to Bao (2000). The basic physiochemical properties of the tested sediments are listed in Table 1.

2.2. Preparation of NZVI and modified NZVI

Ferrous sulfate heptahydrate (99%), sodium borohydride (98.5%), and SA used for the preparation of NZVI and SNZVI were purchased from Jingkang New Material Technology Co., Ltd (Changsha, China). Ultra-pure water (18.2 MΩ cm, Barnstead D11911), ethanol and other solutions were deoxygenated before the reaction by introduction of nitrogen gas. All reagents for the experiments were of reagent grade and all solutions and dilutions were prepared in ultra-pure water.

NZVI nanoparticles were then prepared by reducing Fe^{2+} ions to Fe^{0} using borohydride solution at a BH_4^-/Fe^{2+} molar ratio of 2.0 (He and Zhao, 2007). An aqueous solution of 0.05 M $FeSO_4 \cdot 7H_2O$ was continuously mixed while 0.1 M $NaBH_4$ was added into a three-necked flask meanwhile continuously stirred with mechanical agitator under nitrogen protection, followed by an hour of mixed reaction. After synthesis, nanoparticles were separated magnetically and then washed three times with deoxy ultrapure water and ethanol in order to remove the remaining borohydride and dried under vacuum drying oven (DZF-6020, Shanghai) and stored in brown bottles filled with nitrogen gas.

SNZVI was prepared by dispersing NZVI particles in aqueous SA to result in suspensions comprising iron nanoparticles (0.5 g/L) and SA of various concentrations (0, 0.05, 0.1, 0.15, 0.2 wt%) individually, followed by sonication for 30 min.

2.3. Characterization

SEM images of NZVI and SNZVI were determined using a scanning electron microscope (SEM) (Quanta TM 250, USA). NZVI and SNZVI particle hydrodynamic diameters were determined by dynamic light scattering (DLS) using a Zetasizer Nano ZS (Malvern). Images of the materials were obtained at an accelerating voltage of 20 kV. X-ray diffraction (XRD) patterns of NZVI and SNZVI samples were studied using AXS D8 Advance, LynxEye array detector equipped with Cu-Ka radioactive source (λ=0.154 nm). The angle of diffraction was varied from 10° to 80° at the speed of 2°/min. Fourier transform infrared spectra of NZVI and SNZVI were obtained using 5700 FTIR Spectrometer (NICOLET, USA). 32 scans were taken.

2.4. Experimental design

Different fractions of Cd, enzyme activities and bacterial community diversity were analyzed with sediment samples respectively treated by adding 0.5 g / 2 g / 2 g (dry weight) of sediments and 5 mL/ 20 mL/ 20 mL of the SNZVI (0, 0.05, 0.1, 0.15, 0.2 wt%) suspension in 50 mL centrifuge tubes with screw caps, resulting in a suspension-to-sediment ratio of 10:1 (mL/g) in each sample. The mixtures were sealed and then placed at room temperature (23 ± 1 °C) for aging without any prior pH adjustment. Control experiments with sediment samples were also conducted using ultra-pure water instead of the SNZVI suspensions. For the purpose of investigating the effect of reaction time on Cd-immobilization efficiency, the sediment reaction time was undertaken on day 0, 1, 3, 5, 7, 10, 15, 30 for the analysis of metal fraction and enzyme assays and the diversity of bacterial communities. In order to ensure the quality of the data, all sediment treatments were performed in triplicate.

171 Illustration of the preparation procedure and the whole experiment procedure are
172 presented in Fig. 2.

173 **2.5. Sequential extraction of sediment-sorbed Cd^{2+}**

174 Different fractions of Cd in the samples were determined by the procedure of selective
175 sequential extraction (SSE). The procedure adopted in our experiment was the
176 three-step extraction of the European Measurements (Salomons, 2006). Four different
177 fractions are considered: i) Soluble species, carbonates, cation exchange sites (here
178 after defined as acid-soluble), extracted utilizing 0.11 M acetic acid, pH 2; ii) iron and
179 manganese oxides fraction (i.e. reducible fraction), extracted with 0.5 M
180 hydroxylammonium chloride, pH 2; iii) organic and sulfide fraction (i.e. oxidizable
181 fraction), extracted by hydrogen peroxide 30% and treated with 1 M ammonium
182 acetate at pH 2, and iv) the residual fraction, that remains in the solid (i.e., the metals
183 in the crystalline lattice of primary and secondary minerals), extracted by aqua regia.
184 0.5 g treated sediment was put in a 50 mL Teflon centrifuge tube and the first step of
185 extract fluid mixed with samples of supernatant fluid. For each step, the extract fluid
186 was decanted, filtered through a 0.45 μm filter membrane, and then the filtrate was
187 analyzed for Cd by AAS. All of the extractions were performed in triplicate.

188 **2.6. Enzyme activity assays**

189 Enzyme activity can be used as a good indicator for studying the activity of
190 microorganisms, and it also represents the scope of nutrient cycling and the process of
191 decomposition. Urease activity was assayed with method described by Hu et al. (2014)
192 expressed as NH_4-N mg/g. Catalase activity was analyzed by titration with 0.1 mol/L

193 $KMnO_4$ (Sun et al., 2012), expressed as mL/g. Dehydrogenase (DEH) activity was
194 determined as described by Casida Jr et al. (1964) and the reddish color intensity of
195 the filtrate was measured with a ultraviolet-visible spectrophotometer (UV-2700,
196 SHIMADZU) at a wavelength of 485 nm and methanol was used as a blank. All the
197 enzyme activities assays were applied to the moist sediment samples in triplicate.

198 **2.7. DNA extraction and PCR-DGGE analysis**

199 DNA was extracted from the sediment samples using the Soil DNA Extraction Kit
200 (MoBio Laboratories), according to the manufacture instructions. Previous studies
201 showed that the kit provides estimates of bacterial diversity equal to those obtained
202 using other in situ lysis procedures (Luna et al., 2006). The extracted DNA was stored
203 at -20 °C for future applications. Confirmation of the extraction and integrity of DNA
204 was performed in agarose gel with ethidium bromide staining.

205 Bacterial 16S rRNA genes were amplified by using the universal forward primer
206 PRBA338F (5'-ACTCCTACGGGAGGCAGCAG-3') and PRUN518R (5'-ATTACC
207 GCGGCTGCTGG-3') primers with a GC clamp attached to the forward primer
208 (Ovreås et al., 1997). PCR and DGGE were performed by the method of Liu et al.
209 (2014).

210 **2.8. Statistical analysis**

211 All univariate data were analyzed using the software package SPSS 16.0 (SPSS Inc,
212 Chicago, Illinois, USA). One-way analysis of variance (ANOVA) and Two-way
213 ANOVA were used to determine differences of urease activity, catalase activity,
214 dehydrogenase activity among the treatment groups and individual effect of time and

concentrations. Shannon-Wiener diversity index (H) for bacterial DGGE community fingerprinting calculated as follows:

$$H = -\Sigma\left(\frac{Ni}{N}\right)\ln\left(\frac{Ni}{N}\right) \qquad (1)$$

Where Ni was the height of a peak of each band i, i was the number of bands in each DGGE profile, and N was the sum of all peak heights in a given DGGE profile.

The correlation between the distributions of bacterial communities and the different SNZVI concentrations were assayed by principal component analysis (PCA) using CANOCO software V4.5 (Biometris, Wageningen, Netherlands) (Zhang et al., 2011a).

3. Results and discussion

3.1. Characterization

The SEM images of NZVI and SNZVI showed that the morphology and nanoparticle distribution of NZVI in the absence or presence of SA (Fig. 3). The synthesized NZVI in the absence of SA showed that NZVI particles were aggregated into a chain-like structure (Fig. 3a), that can lead to a decrease of its surface reactivity (He and Zhao, 2005). Therefore Fe^0 nanoparticles are usually fixed on support materials such as resins or starch (He and Zhao, 2005; Li et al., 2007), considering it decreased the aggregation of Fe^0 nanoparticles and improved its mechanical strength. Compared with Fig. 3a, the 0.1 wt% SNZVI presented in Fig. 3b was clearly well-dispersed, and on the surface of the zero-valent iron were spherical particles. The hydrodynamic diameter of the NZVI particles produced was less than 100 nm (Supplementary Materials, Fig. S2a), the distribution consisted primarily (35.1%) of particles 43.82

237 nm in diameter. Fig. S2b (Supplementary Materials) shows the hydrodynamic
238 diameter and size distribution of the 0.1 wt% SNZVI. The particle size of the SNZVI
239 was mainly distributed in the ranging from 107.67 nm to 110.23 nm. It means the
240 particle size distribution is narrower.

241 Fig. 4 presents the XRD pattern of NZVI (a) and synthesized SNZVI (b). The
242 diffraction peak at 44.9° (2θ) as shown in Fig. 4b, corresponded to the formation of
243 iron in its zero-valent form (Weng et al., 2013). This indicated that SA was coated
244 onto the NZVI surface. In addition, iron oxides were detected on the surface of the
245 NZVI: $Fe_3O_4/\gamma\text{-}Fe_2O_3$ morphology corresponding to 2θ at 35° and Fe^0 at 30° (Zhang
246 et al., 2011b; Kanel et al., 2005) were observed in Fig. 4a. However, Fig. 4b shows
247 that these peaks of iron oxides were reduced or disappeared in SNZVI, where ferrous
248 oxide (FeO) magnetite/maghemite ($Fe_3O_4/\gamma\text{-}Fe_2O_3$), and lepidocrocite (γ-FeOOH)
249 were produced in NZVI. These corresponded to the peaks marked as “F”, “M”, “L” in
250 Fig. 4a (Kim et al., 2013; Zhang et al., 2011b). It is suggested that the SA used in the
251 synthesizing procedure might prevent NZVI particles from air oxidating. The
252 characteristic peak of SA (Gong et al., 2016) has not been detected because of its low
253 concentration. Based on these results, it was concluded that the surface of SNZVI
254 offers more stability, which was consistent with results obtained for NZVI supported
255 on materials such as resin, starch, or surfactant modified zeolite (He and Zhao, 2005;
256 Li et al., 2007; Ponder et al., 2000).

257 FTIR spectra for NZVI and SNZVI were scanned in the range of 4000-400 cm^{-1}
258 (Fig. 5), where Fig. 5a and Fig. 5b indicate NZVI and 0.1 wt% SNZVI, respectively.

Broad bands at 3500-3300 cm^{-1} in NZVI and the composite (Fig. 5a and b) resulted from O-H stretching may be attributed to H_2O and M-OH, while the band at 1650 cm^{-1} can be due to O-H bending (Mohapatra et al., 2010). Strong bands at < 900 cm^{-1} in the NZVI alone (Fig. 5a), attributable in part to the presence of iron oxidation oxides (Zhang et al., 2011b), were weaker in the composite, indicating less oxidation of SNZVI. The SA support may reduce the generation of iron oxide. In addition, Fe-O stretches of Fe_2O_3 and Fe_3O_4 were observed at 469.00 cm^{-1} and 540.60 cm^{-1}, which demonstrated much consistency with the NZVI FTIR spectra in Fig. 5a. Combined with the results from FTIR and XRD, it indicated that NZVI had been successfully coated by SA where the surface of the coated NZVI was partially oxidized.

3.2. Changes in Cd partitioning

The total concentration of Cd in the sediments was 20.90 ± 0.67 (mg/kg). The concentration of Cd in the sediments was much higher than the effects range low (ERL) value (1.2 mg/kg) recommended by the sediment quality guideline (Burton et al., 2002). However, total Cd concentrations do not necessarily correspond with metal bioavailability in natural systems (Sun et al., 2016). Speciation of the metal ion in the sediment may play a significant role on its bioavailability (Fonti et al., 2015). To highlight and better understand the effect of nanoparticles on the changes of metal distribution and to evaluate the level of their stabilization, fractionation of Cd in the sediment was performed. In general, the mobility and availability of Cd increases in the order of acid-soluble forms> reducible forms> oxidizable forms> residual forms (Soylak, 2015). Changes in metal fraction because of SNZVI applications were

already confirmed after 30 d of incubation (Fig. 6a), and significant changes on distribution of metal forms in the sediment was noted. In all cases, a general increase in the residual fraction was observed with adding SNZVI (NZVI modified with SA of various concentrations from 0, 0.05, 0.1, 0.15, 0.2 wt%). The residual fractions in the sediment were of durable solid phase and not easy to be extracted and residual metal complexes (metals within the structure of the sediment and minerals) have been considered as inert and inaccessible to biota (Obst and Steinbüchel, 2004). It was found that the presence of NZVI, 0.05 wt% SNZVI, 0.1 wt% SNZVI ,0.15 wt% SNZVI, 0.2 wt% SNZVI increased the residual fraction of Cd from initial 5.26, 3.74, 5.0, 4.75, 4.33 mg/kg to 10.84, 11.47, 11.97, 11.46, 11.08 mg/kg and the corresponding residual fraction percentages of Cd increased from 25.17%, 17.90%, 23.99%, 22.76%, 20.72% to 51.89%, 54.90%, 57.28%, 54.87%, 53.02% after 30 days of incubation, respectively (Fig. 6b). Compared to no-amended sediment, the residual fraction percentage of Cd after applying different concentrations of SNZVI was increased from 36.42% to 41.80%. With an increasing concentration of SA from 0.1 wt% to 0.2 wt%, it did not increase further but decreased to some degree. It was presumed that the decrease in negative surface charge with an increasing concentration of SA might be ascribed to the entanglement or cross-linking of the SA molecules on the surface of SNZVI (Dong et al., 2016; Lin et al., 2010). In addition, we tested the fractions of Cd after 90 d incubating. It was found that the corresponding residual fraction percentages of Cd decreased from 51.89%, 54.90%, 57.28%, 54.87%, 53.02% to 49.03%, 50.83%, 53.92%, 51.80%, 50.05% after 90 days

303 of incubation, respectively (Supplementary Materials, Fig. S3). Few metals were
304 desorbed from Cd in fraction i, ii, iii in sediments treated with SNZVI even after 90
305 days (Wen et al., 2016). The findings showed that the stabilization of SNZVI was
306 quite durable and using the modified NZVI is a possible solution to alleviate the
307 hazards likely posed to the river and the surrounding environment. Wen et al. (2016)
308 used modified zeolite to immobilize Cd in sediment, and reported that the residual
309 fraction of Cd was significantly increased by 8.3%. Zhang et al. (2010) reported that
310 nano-hydroxyapatite can immobilize Cd in sediment effectively, and the residual
311 fraction of Cd increased from 29.1 (0% addition) to 41.8 (10% addition) after 14 days
312 of remediation. It can greatly weaken the release of metals to the environment by
313 decreasing the active Cd fractions in spite of the unable removal of metals from
314 sediments, the same as the accepted application of zeolites or other materials to the
315 remediation of metal contaminated sediments (Wen et al., 2016; Zhang et al., 2010).
316 The reasons that can be accounted for metal stabilization in sediment using
317 modified NZVI: Firstly, during NZVI preparation, iron oxidation produces surface
318 hydroxides in proximity to FeOOH (Sun et al., 2006). The immobilization of Cd^{2+} by
319 SNZVI appears to involve a diffusion of metal ions to SNZVI particles and surface
320 complexation of Cd^{2+} with iron hydroxides. The surface reactions of Cd
321 immobilization by NZVI may be described by the following equations (Zhang et al.,
322 2014):

323 $$FeOH + Cd^{2+} + H_2O \rightarrow FeOCdOH + 2H^+ \qquad (2)$$

324 In addition, each monomeric unit of SA contains one carboxylate and two hydroxyl

groups. And the hydroxyl and Cd combine to form $Cd(OH)^+$, which is adsorbed onto SNZVI or the structure of FeOOH (Zhang et al., 2014). Previous studies showed that Cd was stoichiometrically coprecipitated with Fe(III) (oxyhydr)oxides (Muehe et al., 2013).

3.3. Enzyme activities

Fig. $7a_1$ shows the changes of urease activities with different SNZVI concentrations in sediments during incubation time. It increased with SNZVI (0, 0.05, 0.1, 0.15, 0.2 wt%) and varied as the incubation proceeded. After 30 d of incubation, this enzyme activity increased 3.80, 4.03, 4.73, 4.42, 4.34 times higher than that of the unamended sediment with NZVI, 0.05 wt% SNZVI, 0.1 wt% SNZVI, 0.15 wt% SNZVI, 0.2 wt% SNZVI treatments, respectively. It was observed that the urease activities in the sediment increased significantly after 10 days' of incubation. Moreover, urease activity was higher in various SA treatments than in the control of no adding SA. The aging phenomenon was observed, because the adsorption of Cd to SNZVI changed the fraction of Cd into residual forms, and thus decreased the bioavailability of Cd. Previous research has shown that enzyme activity increased with available contents of heavy metals decreasing (Wang et al., 2007).

The sensitivities of catalase to different levels of SNZVI in sediments were shown in Fig. $7b_1$. The catalase activity increased slightly with the increasing of incubation periods. This enzyme was higher in various SNZVI treatments compared to the control. In the presence of 0.1 wt% SNZVI, the enzymes activities were slightly higher than those in other concentrations on day 30, and the catalase activity was 1.78

347 times higher than that of the unamended sediment.

348 Dehydrogenase activity decreased significantly with SNZVI of different
349 concentrations in the amended samples in Fig. $7c_1$. This enzyme activity of the control
350 group was significantly lower than in treatments and the image of control was not
351 shown in Fig. $7c_1$, because it is not visible beside the other results. The inhibition of
352 dehydrogenase by SNZVI indicated that it may not be very useful for the evaluation
353 of sediments recovery under Cd pollution. Although it showed a downward trend, the
354 dehydrogenase activity was still higher than that of the original sediment. Exclusive
355 of dehydrogenase, the activities of the other two enzymes tested were enhanced with
356 the increase of incubation time. For this reason, according to several previous studies
357 (Menon et al., 2005; Stêpniewski et al., 2000), we concluded that dehydrogenase
358 might be inhibited by ferric ions formed from SNZVI whereas no obvious inhibition
359 was found against other enzymes. Generally, applications of SNZVI increased
360 sediment enzymatic activities. Compared with unamended sediment, urease, catalase,
361 and dehydrogenase activities under SNZVI treatments were enhanced by 3.8-4.73,
362 1.29-1.78 and 134.32-297.51 times, respectively. It was clearly observed from Fig. $7a_2$,
363 Fig. $7b_2$, and Fig. $7c_2$ that the activities of the enzymes tested increased multiples
364 compared with the control sediment after 30 d incubation, respectively. Statistical
365 analysis of data by one-way ANOVA and two-way ANOVA showed urease, catalase,
366 dehydrogenase that indicated significant differences ($P < 0.05$ or $P < 0.01$) in
367 incubation time and different SNZVI concentrations (Table 2). Significant interaction
368 effects of both time and concentrations on the activities of the enzymes tested were

observed statistically (Table 2).

3.4. PCR-DGGE for bacterial community structure

PCR-DGGE was used to investigate the structural diversity of bacterial communities under SNZVI treatments of different concentrations on day 30. DNA was extracted from the Cd-contaminated samples and the DGGE patterns of PCR-amplified 16S rRNA were shown in Fig. 8. In these samples, the PCR-DGGE patterns indicated a greater complexity of banding pattern about bacterial community structure at 0.1% wt SA than at other concentrations, resulting in a high number of different bacterial taxa emerging. While the bacterial DGGE profiles of 16S rRNA gene fragments from different SA-treated sediments were generally similar, indicating that the microbes with those bands were stable and little influenced by SA. However, there were a few bands emerged after SNZVI treatments. The DGGE profile showed that the structure of bacterial community was changed after 30 d of incubation, particularly at 0.1% wt SA concentration. Similarity dendrograms and phylogenetic analysis showed by the image analysis of DGGE combined with the Dice similarity coefficient indicated that PCR-DGGE patterns of SNZVI treated samples could be well distinguished from the control group (Fig. 8), indicating that many common microbial members were still presented in each treatment. The DGGE gel profiles were further visualized by the Shannon-Wiener diversity index (H), which provided a direct indication of the apparent diversity of a microbial community (Fig. 9). The experimental groups showed more abundance and diversity of bacteria. The Shannon diversity of the bacteria reached the peak in sample 4.

In an attempt to explain the effects of different concentrations of SNZVI on the indigenous microorganisms, we performed a principal component analysis (PCA) of the results from the sediment samples. The results were shown in Fig. 10. The sample (1, 2, 3, 4, 5, 6) represents the different concentrations of SA (0, 0.05, 0.1, 0.15, 0.2 wt%). The cumulative contribution rate of the two principal components (52.1 and 28.1 % for PC1 and PC2, respectively) reached 80.2%. The PCA results clearly indicated that the bacterial community structure has changed obviously in the sediment after the SNZVI application, and the change was determined by the SA concentrations. On one hand, it was noticed that the sediment samples were divided into 4 groups. PC1 exhibited positive correlation with the sample 1, 2 and 5 and PC2 exhibited positive correlation with the sample 1 and 3. But PC1 and PC2 had exhibited negative correlation with the sample 4 and 6. On the other hand, the bands were mostly concentrated in the 2^{nd} and 3^{rd} quadrant and the sample 3, 4 and 6 were also in these two quadrants, indicating the high correlation between these samples and these bands, and showing that these bands represented the bacterial species were main species in these samples.

Microbial populations have complex interactions, such as association and competition (Diao and Yao., 2009). Effects of heavy metals were not only observed on the microbial species, but also on the microbial populations in the sediment (Němeček et al., 2014). SA was such a biodegradable polymer that certain bacteria were able to hydrolyze it (Obst and Steinbüchel, 2004), improving the bioavailability of carbon and nitrogen. Increase in bacterial abundance shows that the

413 microorganisms can use SA as a nutrient source since the system was carbon or
414 nitrogen limited. But the degradation of polymers by bacteria often requires the
415 molecule to be drawn into the cell membrane (Kawai, 2010). Since nanoparticles
416 larger than 10 nm may not be internalized by bacteria with intact membranes (Neal,
417 2008), it is not probable that biodegradable polymers can be transformed when
418 covalently bound to a nanoparticle. Although polymers are biodegradable (Kaplan et
419 al., 1979), the time scales are particularly slow (on the order of 1% degradation over
420 80 days). Previous studies have shown that addition of polyaspartate coated NZVI did
421 not decrease the count of total bacteria and also found that the polymer coating can be
422 bioavailable when bonded to a nanoparticle (Kirschling et al., 2011).

423 **4. Conclusions**

424 In this study, characterization with SEM, DLS, FTIR and XRD analyses demonstrated
425 that the presence of SA led to a decrease in aggregation of iron nanoparticles and a
426 small number of iron oxides formed on the surface of SNZVI. The findings have
427 shown that the addition of SNZVI was effective in immobilizing Cd in polluted
428 sediments, resulting in an increased (or a bigger) residual fraction of Cd and a
429 decrease of the bioavailability of Cd. Moreover, the increase of enzymes activities
430 (urease, catalase, and dehydrogenase) and bacterial community diversity indicated the
431 recovery of metabolic function to some extent by adding SNZVI of different
432 concentrations. Additionally, these results could probably provide a reference for risk
433 assessments of using NZVI particles for sediment remediation and of using surface
434 coatings on these nanoparticles.

435 However, as noted in our study, this nanotechnology still has its limitations. It is
436 possible that Cd become remobilized due to long-term processes or changes of the
437 environmental conditions change (Calderon and Fullana, 2015). And the heavy metals
438 existing in inactive form still remain in sediment. In addition, further studies are
439 needed to reveal the potential effects of SNZVI application on other metals in
440 contaminated sediments.

441 **Acknowledgements**

442 This study was financially supported by the Program for the National Natural Science
443 Foundation of China (51378190, 51278176, 51408206, 51579098, 51521006), the
444 National Program for Support of Top-Notch Young Professionals of China (2014), the
445 Fundamental Research Funds for the Central Universities, the Program for New
446 Century Excellent Talents in University (NCET-13-0186), the Program for
447 Changjiang Scholars and Innovative Research Team in University (IRT-13R17),
448 Scientific Research Fund of Hunan Provincial Education Department
449 (No.521293050).

450 **Supplementary data**

451 This file contains additional Fig. S1-S3 and Table S1.

452 **References**

453 Akcay, H., Oguz, A., Karapire, C., 2003. Study of heavy metal pollution and
454 speciation in Buyak Menderes and Gediz river sediments. Water Research 37 (4),
455 813-822.

456 Aydin, S., Shahi, A., Ozbayram, E.G., Ince, B. and Ince, O., 2015. Use of PCR-DGGE

based molecular methods to assessment of microbial diversity during anaerobic treatment of antibiotic combinations. Bioresource Technology 192, 735-740.

Bao, S.D., 2000. Soil and Agricultural Chemistry Analysis, third ed. Press of China Agricultural, Beijing.

Borba, P.A.A., Pinotti, M., de Campos, C.E.M., Pezzini, B.R., Stulzer, H.K., 2016. Sodium alginate as a potential carrier in solid dispersion formulations to enhance dissolution rate and apparent water solubility of BCS II drugs. Carbohydrate Polymers 137, 350-359.

Burton Jr, G.A., 2002. Sediment quality criteria in use around the world. Limnology 3 (2), 65-76.

Casida Jr, L., Klein, D. and Santoro, T., 1964. Soil dehydrogenase activity. Soil Science 98 (6), 371-376.

Calderon, B. and Fullana, A., 2015. Heavy metal release due to aging effect during zero valent iron nanoparticles remediation. Water Research 83, 1-9.

Cumbal, L., Greenleaf, J., Leun, D. and SenGupta, A.K., 2003. Polymer supported inorganic nanoparticles: characterization and environmental applications. Reactive and Functional Polymers 54 (1), 167-180.

De Jonge, M., Teuchies, J., Meire, P., Blust, R., Bervoets, L., 2012. The impact of increased oxygen conditions on metal-contaminated sediments part I: Effects on redox status, sediment geochemistry and metal bioavailability. Water Research 46 (7), 2205-2214.

Diao, M. and Yao, M., 2009. Use of zero-valent iron nanoparticles in inactivating

479 microbes. Water Research 43 (20), 5243-5251.

480 Dong, H. and Lo, I.M., 2013. Influence of humic acid on the colloidal stability of

481 surface-modified nano zero-valent iron. Water Research 47 (1), 419-427.

482 Dong, H., Xie, Y., Zeng, G., Tang, L., Liang, J., He, Q., Zhao, F., Zeng, Y., Wu, Y.,

483 2016. The dual effects of carboxymethyl cellulose on the colloidal stability and

484 toxicity of nanoscale zero-valent iron. Chemosphere 144, 1682-1689.

485 Dror, I., Jacov, O.M., Cortis, A., Berkowitz, B., 2012. Catalytic transformation of

486 persistent contaminants using a new composite material based on nanosized

487 zero-valent iron. ACS Applied Materials & Interfaces 4 (7), 3416-3423.

488 Fassett, D.W., 1975. Cadmium: Biological effects and occurrence in the environment.

489 Annual review of Pharmacology 15 (1), 425-435.

490 Feng, Y., Gong, J., Zeng, G., Niu, Q., Zhang, H., Niu, C., Deng, J., Yan, M., 2010.

491 Adsorption of Cd (II) and Zn (II) from aqueous solutions using magnetic

492 hydroxyapatite nanoparticles as adsorbents. Chemical Engineering Journal 162

493 (2), 487-494.

494 Fonti, V., Beolchini, F., Rocchetti, L. and Dell'Anno, A., 2015. Bioremediation of

495 contaminated marine sediments can enhance metal mobility due to changes of

496 bacterial diversity. Water Research 68, 637-650.

497 Gong, X., Branford-White, C., Tao, L., Li, S., Quan, J., Nie, H. and Zhu, L., 2016.

498 Preparation and characterization of a novel sodium alginate incorporated

499 self-assembled Fmoc-FF composite hydrogel. Materials Science and Engineering:

500 C 58, 478-486.

501 Hakanson, L., 1980. An ecological risk index for aquatic pollution control. A
502 sedimentological approach. Water Research 14 (8), 975-1001.
503 He, F. and Zhao, D., 2005. Preparation and characterization of a new class of
504 starch-stabilized bimetallic nanoparticles for degradation of chlorinated
505 hydrocarbons in water. Environmental Science & Technology 39 (9), 3314-3320.
506 He, F. and Zhao, D., 2007. Manipulating the size and dispersibility of zerovalent iron
507 nanoparticles by use of carboxymethyl cellulose stabilizers. Environmental
508 Science & Technology 41 (17), 6216-6221.
509 Huang, D., Wang, R., Liu, Y., Zeng, G., Lai, C., Xu, P., Lu, B., Xu, J., Wang, C.,
510 Huang, C., 2015. Application of molecularly imprinted polymers in wastewater
511 treatment: a review. Environmental Science and Pollution Research 22 (2),
512 963-977.
513 Hu, B., Liang, D., Liu, J., Lei, L. and Yu, D., 2014. Transformation of heavy metal
514 fractions on soil urease and nitrate reductase activities in copper and selenium
515 co-contaminated soil. Ecotoxicology and Environmental Safety 110, 41-48.
516 Jain, C., 2004. Metal fractionation study on bed sediments of River Yamuna, India.
517 Water Research 38 (3), 569-578.
518 Kanel, S.R., Manning, B., Charlet, L. and Choi, H., 2005. Removal of arsenic (III)
519 from groundwater by nanoscale zero-valent iron. Environmental Science &
520 Technology 39 (5), 1291-1298.
521 Kaplan, D., Hartenstein, R. and Sutter, J., 1979. Biodegradation of polystyrene, poly
522 (metnyl methacrylate), and phenol formaldehyde. Applied and environmental

523 microbiology 38 (3), 551-553.

524 Kawai, F., 2010. The biochemistry and molecular biology of xenobiotic polymer
525 degradation by microorganisms. Bioscience, biotechnology, and biochemistry 74
526 (9), 1743-1759.

527 Kharisov, B.I., Dias, H.R., Kharissova, O.V., Jiménez-Pérez, V.M., Perez, B.O.,
528 Flores, B.M., 2012. Iron-containing nanomaterials: synthesis, properties, and
529 environmental applications. RSC Advances 2 (25), 9325-9358.

530 Kim, S.A., Kamala-Kannan, S., Lee, K.-J., Park, Y.-J., Shea, P.J., Lee, W.-H., Kim,
531 H.-M., Oh, B.-T., 2013. Removal of Pb (II) from aqueous solution by a zeolite –
532 nanoscale zero-valent iron composite. Chemical Engineering Journal 217, 54-60.

533 Kim, H.-J., Phenrat, T., Tilton, R.D. and Lowry, G.V., 2009. Fe^0 nanoparticles remain
534 mobile in porous media after aging due to slow desorption of polymeric surface
535 modifiers. Environmental Science & Technology 43 (10), 3824-3830.

536 Kirschling, T.L., Golas, P.L., Unrine, J.M., Matyjaszewski, K., Gregory, K.B., Lowry,
537 G.V., Tilton, R., D., 2011. Microbial bioavailability of covalently bound polymer
538 coatings on model engineered nanomaterials. Environmental Science &
539 Technology 45 (12), 5253-5259.

540 Kumpiene, J., Ore, S., Renella, G., Mench, M., Lagerkvist, A., Maurice, C., 2006.
541 Assessment of zerovalent iron for stabilization of chromium, copper, and arsenic
542 in soil. Environmental pollution 144 (1), 62-69.

543 Lin, Y., Tseng, H., Wey, M., Lin, M., 2010. Characteristics of two types of stabilized
544 nano zero-valent iron and transport in porous media. Science of the Total

545 Environment 408 (10), 2260-2267.

546 Liu, R., Xiao, N., Wei, S., Zhao, L., An, J., 2014. Rhizosphere effects of

547 PAH-contaminated soil phytoremediation using a special plant named Fire

548 Phoenix. Science of the Total Environment 473, 350-358.

549 Li, Z., Jones, H.K., Zhang, P. and Bowman, R.S., 2007. Chromate transport through

550 columns packed with surfactant-modified zeolite/zero valent iron pellets.

551 Chemosphere 68 (10), 1861-1866.

552 Luna, G.M., Dell'Anno, A. and Danovaro, R., 2006. DNA extraction procedure: a

553 critical issue for bacterial diversity assessment in marine sediments.

554 Environmental Microbiology 8 (2), 308-320.

555 Menon, P., Gopal, M., Parsad, R., 2005. Effects of chlorpyrifos and quinalphos on

556 dehydrogenase activities and reduction of Fe^{3+} in the soils of two semi-arid fields

557 of tropical India. Agriculture, Ecosystems & Environment 108 (1), 73-83.

558 Mohapatra, M., Mohapatra, L., Singh, P., Anand, S. and Mishra, B.K., 2010. A

559 comparative study on Pb(II), Cd(II), Cu(II), Co(II) adsorption from single and

560 binary aqueous solutions on additive assisted nano-structured goethite.

561 International Journal of Engineering Science & Technology 2 (8).

562 Muehe, E.M., Adaktylou, I.J., Obst, M., Zeitvogel, F., Behrens, S., Planer-Friedrich,

563 B., Kraemer, U. and Kappler, A., 2013. Organic carbon and reducing conditions

564 lead to cadmium immobilization by secondary Fe mineral formation in a

565 pH-neutral soil. Environmental Science & Technology 47 (23), 13430-13439.

566 Neal, A.L., 2008. What can be inferred from bacterium-nanoparticle interactions

about the potential consequences of environmental exposure to nanoparticles? Ecotoxicology 17 (5), 362-371.

Němeček, J., Lhotský, O. and Cajthaml, T., 2014. Nanoscale zero-valent iron application for in situ reduction of hexavalent chromium and its effects on indigenous microorganism populations. Science of the Total Environment 485-486 (1), 739-747.

Obst, M. and Steinbüchel, A., 2004. Microbial degradation of poly (amino acid) s. Biomacromolecules 5 (4), 1166-1176.

Olivares-Rieumont, S., De la Rosa, D., Lima, L., Graham, D.W., Katia, D., Borroto, J., Martínez, F., Sánchez, J., 2005. Assessment of heavy metal levels in Almendares River sediments—Havana City, Cuba. Water Research 39 (16), 3945-3953.

Ovreås, L., Forney, L., Daae, F.L. and Torsvik, V., 1997. Distribution of bacterioplankton in meromictic Lake Saelenvannet, as determined by denaturing gradient gel electrophoresis of PCR-amplified gene fragments coding for 16S rRNA. Applied and environmental microbiology 63 (9), 3367-3373.

Peng, J.F., Song, Y.H., Yuan, P., Cui, X.Y. and Qiu, G.L., 2009. The remediation of heavy metals contaminated sediment. Journal of hazardous materials 161 (2-3), 633-640.

Ponder, S.M., Darab, J.G., Mallouk, T.E., 2000. Remediation of Cr(VI) and Pb(II) aqueous solutions using nanoscale zerovalent iron. Environmental Science & Technology 34 (12), 2564-2569

Prica, M., Dalmacija, B., Dalmacija, M., Agbaba, J., Krcmar, D., Trickovic, J.,

589 Karlovic, E., 2010. Changes in metal availability during sediment oxidation and
590 the correlation with the immobilization potential. Ecotoxicology and
591 Environmental Safety 73 (6), 1370-1377.
592 Ruttens, A., Adriaensen, K., Meers, E., De Vocht, A., Geebelen, W., Carleer, R.,
593 Mench, M., Vangronsveld, J., 2010. Long-term sustainability of metal
594 immobilization by soil amendments: cyclonic ashes versus lime addition.
595 Environmental pollution 158 (5), 1428-1434.
596 Salomons, W., 2006. Adoption of common schemes for single and sequential
597 extractions of trace metal in soils and sediments.International journal of
598 environmental analytical chemistry 51 (51), 3-4.
599 Sirk, K.M., Saleh, N.B., Phenrat, T., Kim, H.-J., Dufour, B., Ok, J., Golas, P.L.,
600 Matyjaszewski, K., Lowry, G.V. and Tilton, R.D., 2009. Effect of adsorbed
601 polyelectrolytes on nanoscale zero valent iron particle attachment to soil surface
602 models. Environmental Science & Technology 43 (10), 3803-3808.
603 Stêpniewski, W., Stêpniewska, Z., Gliński, J., Brzeziñska, M., Wlodarczyk, T.,
604 Przywara, G., Varallyay, G., Rajkai, K., 2000. Dehydrogenase activity of some
605 Hungarian soils as related to their water and aeration status. International
606 Agrophysics 14 (1), 17-31.
607 Soylak, M., 2015. Characterization of Heavy Metal Fractions in Agricultural Soils by
608 Sequential Extraction Procedure: The Relationship Between Soil Properties and
609 Heavy Metal Fractions. Soil & Sediment Contamination 24 (1), 1-15.
610 Su, Y., Adeleye, A.S., Huang, Y., Sun, X., Dai, C., Zhou, X., Zhang, Y. and Keller,

611 A.A., 2014. Simultaneous removal of cadmium and nitrate in aqueous media by
612 nanoscale zerovalent iron (nZVI) and Au doped nZVI particles. Water Research
613 63, 102-111.
614 Su, Y., Adeleye, A.S., Keller, A.A., Huang, Y., Dai, C., Zhou, X. and Zhang, Y., 2015.
615 Magnetic sulfide-modified nanoscale zerovalent iron (S-nZVI) for dissolved
616 metal ion removal. Water Research 74, 47-57.
617 Sun, Y.P., Li, X.Q., Cao, J., Zhang, W.X. and Wang, H.P., 2006. Characterization of
618 zero-valent iron nanoparticles. Advances in Colloid & Interface Science 120 (1-3),
619 47-56.
620 Sun, Y., Sun, G., Xu, Y., Wang, L., Lin, D., Liang, X. and Shi, X., 2012. In situ
621 stabilization remediation of cadmium contaminated soils of wastewater irrigation
622 region using sepiolite. Journal of Environmental Sciences 24 (10), 1799-1805.
623 Sun, Y., Xu, Y., Xu, Y., Wang, L., Liang, X. and Li, Y., 2016. Reliability and stability
624 of immobilization remediation of Cd polluted soils using sepiolite under pot and
625 field trials. Environmental pollution 208, 739-746.
626 US EPA. 3050B., 1996. Acid Digestion of Sediments, Sludges, and Soils.
627 Vinodhini, R., Narayanan, M., 2008. Bioaccumulation of heavy metals in organs of
628 fresh water fish Cyprinus carpio (Common carp). International Journal of
629 Environmental Science & Technology 5 (2), 179-182.
630 Wang, Y., Shi, J., Wang, H., Lin, Q., Chen, X. and Chen, Y., 2007. The influence of
631 soil heavy metals pollution on soil microbial biomass, enzyme activity, and
632 community composition near a copper smelter. Ecotoxicology and

633 Environmental Safety 67 (1), 75-81.

634 Weng, X., Lin, S., Zhong, Y. and Chen, Z., 2013. Chitosan stabilized bimetallic Fe/Ni
635 nanoparticles used to remove mixed contaminants-amoxicillin and Cd (II) from
636 aqueous solutions. Chemical Engineering Journal 229, 27-34.

637 Wen, J., Yi, Y. and Zeng, G., 2016. Effects of modified zeolite on the removal and
638 stabilization of heavy metals in contaminated lake sediment using BCR
639 sequential extraction. Journal of environmental management 178, 63-69.

640 Xu, P., Zeng, G., Huang, D., Feng, C., Hu, S., Zhao, M., Lai, C., Wei, Z., Huang, C.,
641 Xie, G., 2012. Use of iron oxide nanomaterials in wastewater treatment: a review.
642 Science of the Total Environment 424, 1-10.

643 Zeng, G., Zhang, C., Huang, G., Yu, J., Wang, Q., Li, J., Xi, B. and Liu, H., 2006.
644 Adsorption behavior of bisphenol A on sediments in Xiangjiang River,
645 Central-south China. Chemosphere 65 (9), 1490-1499.

646 Zhang, C., Lai, C., Zeng, G., Huang, D., Tang, L., Yang, C., Zhou, Y., Qin, L., Cheng,
647 M., 2016a. Nanoporous Au-based chronocoulometric aptasensor for amplified
648 detection of Pb^{2+} using DNAzyme modified with Au nanoparticles. Biosensors
649 and Bioelectronics 81, 61-67.

650 Zhang, C., Lai, C., Zeng, G., Huang, D., Yang, C., Wang, Y., Zhou, Y. and Cheng, M.,
651 2016b. Efficacy of carbonaceous nanocomposites for sorbing ionizable antibiotic
652 sulfamethazine from aqueous solution. Water Research 95, 103-112.

653 Zhang, Z., Li, M., Chen, W., Zhu, S., Liu, N. and Zhu, L., 2010. Immobilization of
654 lead and cadmium from aqueous solution and contaminated sediment using

655 nano-hydroxyapatite. Environmental pollution 158 (2), 514-519.

656 Zhang, J., Zeng, G., Chen, Y., Yu, M., Yu, Z., Li, H., Yu, Y., Huang, H., 2011a. Effects

657 of physico-chemical parameters on the bacterial and fungal communities during

658 agricultural waste composting. Bioresource Technology 102 (3), 2950-2956.

659 Zhang, Y., Li, Y., Dai, C., Zhou, X. and Zhang, W., 2014. Sequestration of Cd (II)

660 with nanoscale zero-valent iron (nZVI): Characterization and test in a two-stage

661 system. Chemical Engineering Journal 244 (244), 218 - 226.

662 Zhang, X., Lin, S., Chen, Z., Megharaj, M., Naidu, R., 2011b. Kaolinite-supported

663 nanoscale zero-valent iron for removal of Pb^{2+} from aqueous solution: reactivity,

664 characterization and mechanism. Water Research 45 (11), 3481-3488.

665 Zhang S, Dong WJ, Zhang LC, Chen XB., 1989. Geochemical characteristics of

666 heavy metals in the Xiangjiang River, China. Hydrobiologia 176 (177): 253–262

667 Zhang, Q., Li, Z., Zeng, G., Li, J., Fang, Y., Yuan, Q., Wang, Y. and Ye, F., 2009.

668 Assessment of surface water quality using multivariate statistical techniques in

669 red soil hilly region: a case study of Xiangjiang watershed, China.

670 Environmental monitoring and assessment 152 (1-4), 123-131.

671 Zhou, Q., Wu, Z., Cheng, S., He, F. and Fu, G., 2005. Enzymatic activities in

672 constructed wetlands and di-n-butyl phthalate (DBP) biodegradation. Soil

673 Biology and Biochemistry 37 (8), 1454-1459.

674 Zia, K.M., Zia, F., Zuber, M., Rehman, S., Ahmad, M.N., 2015. Alginate based

675 polyurethanes: A review of recent advances and perspective. International

676 Journal of Biological Macromolecules 79, 377-387.

677 Zou, Y., Wang, X., Khan, A., Wang, P., Liu, Y., Alsaedi, A., Hayat, T. and Wang, X.,
678 2016. Environmental Remediation and Application of Nanoscale Zero-Valent
679 Iron and Its Composites for the Removal of Heavy Metal Ions: A Review.
680 Environmental Science & Technology 50 (14), 7290-7304.

Table 1 - The main characteristics of the sediment.

Depth (cm) 0-20 cm			Mean ± standard deviation (n=3)		
pH			7.79 ± 0.03		
Organic carbon (g/kg)			7.88 ± 0.90		
Organic matter (g/kg)			13.57 ± 1.54		
Water (%)			55.75 ± 0.55		
CEC (cmol/kg)			13.62 ± 3.58		
Moisture content (%)			58.72 ± 0.79		
Total nitrogen (g/kg)			2.16 ± 0.04		
Total phosphoeus (g/kg)			0.17 ± 0.20		
Element	Total content (mg/kg)	Acid-soluble	Reducible	Oxidizable	Residual
Pb	167.10 ± 1.33	4.11%	15.41%	9.45%	71.03%
Cu	69.35 ± 1.60	5.20%	6.39%	19.69%	68.72%
Cr	159.90 ± 0.92	13.09%	4.17%	10.33%	72.41%
Cd	20.90 ± 0.67	49.23%	27.07%	8.21%	15.49%

Table 2 - ANOVA analysis of enzyme activities in Cd polluted sediment with different SNZVI concentrations and incubation time as two main effects.

	One-way ANOVA			Two-way ANOVA		
Facor	Urease	Catalase	Dehydrogenase	Urease	Catalase	Dehydrogenase
Concentration	0.033*	0.004**	0.01**	0.00**	0.00**	0.00**
incubation time	0.00**	0.00**	0.00**			

* Significant differences at the 0.05 level ($p < 0.05$).

** Significant differences at the 0.01 level ($p < 0.01$).

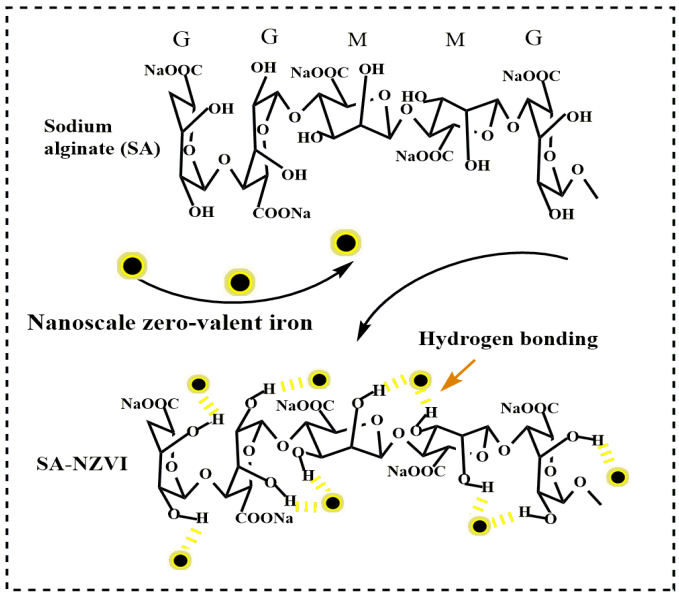

Fig. 1 - Molecular structures of sodium alginate (SA) and the schematic diagram of SA modified NZVI.

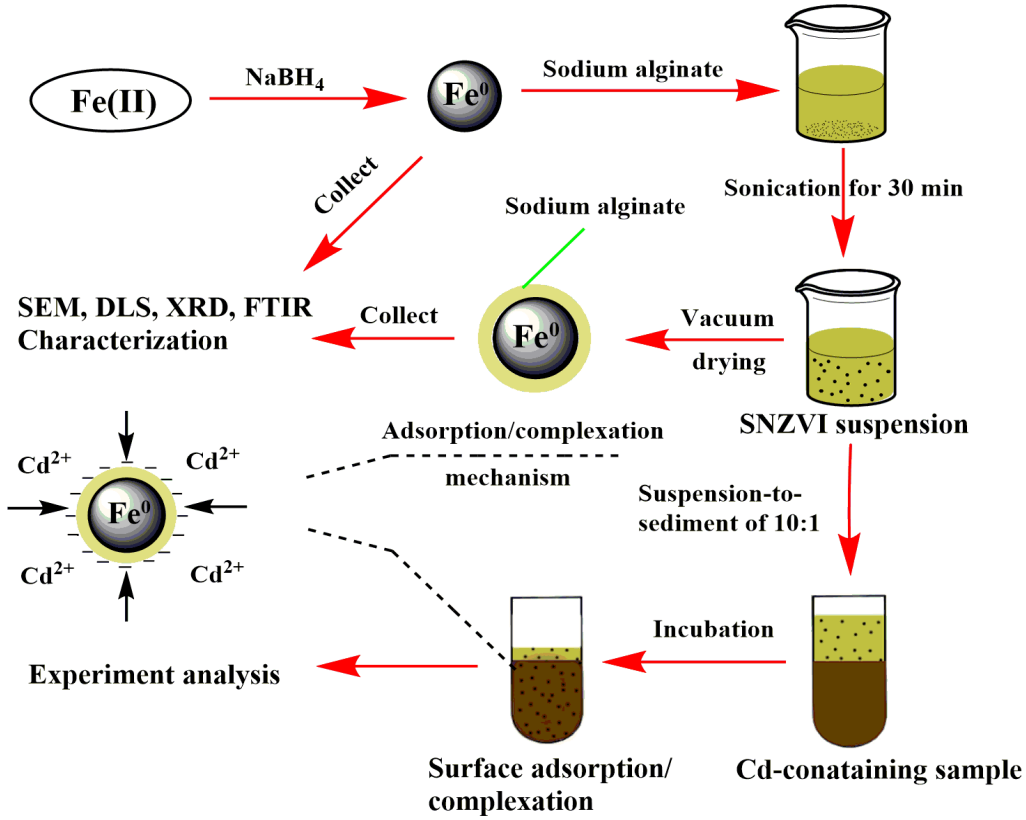

Fig. 2 - Schematics of the preparation of sodium alginate (SA) modified NZVI and their application for adsorption of Cd^{2+}.

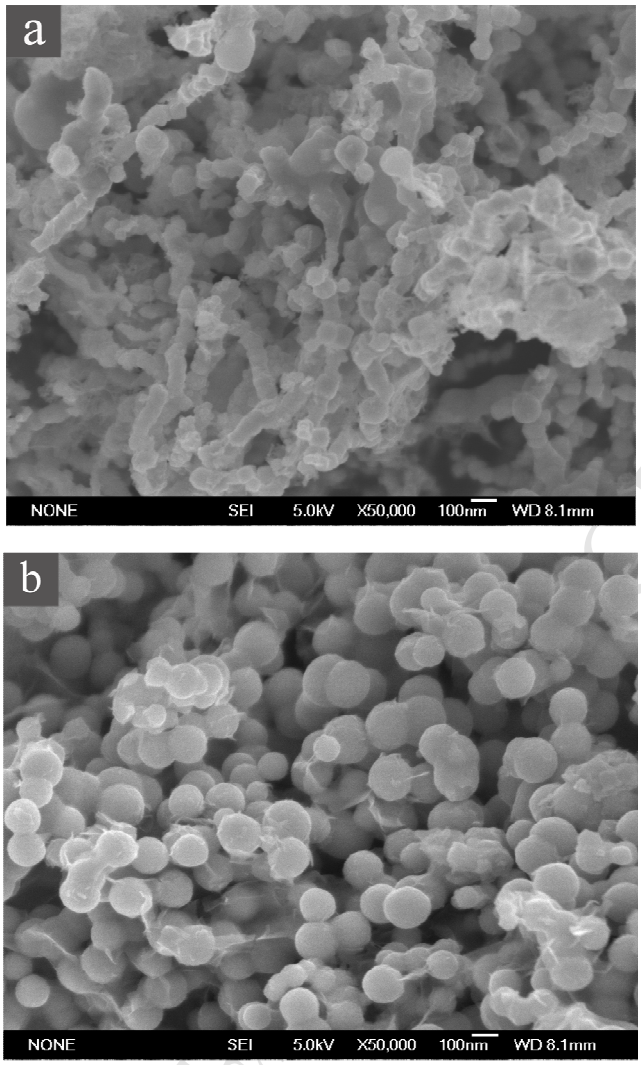

Fig. 3 - SEM images of laboratory synthesized iron particles with and without a modify material. a. NZVI; b. 0.1 wt% SNZVI.

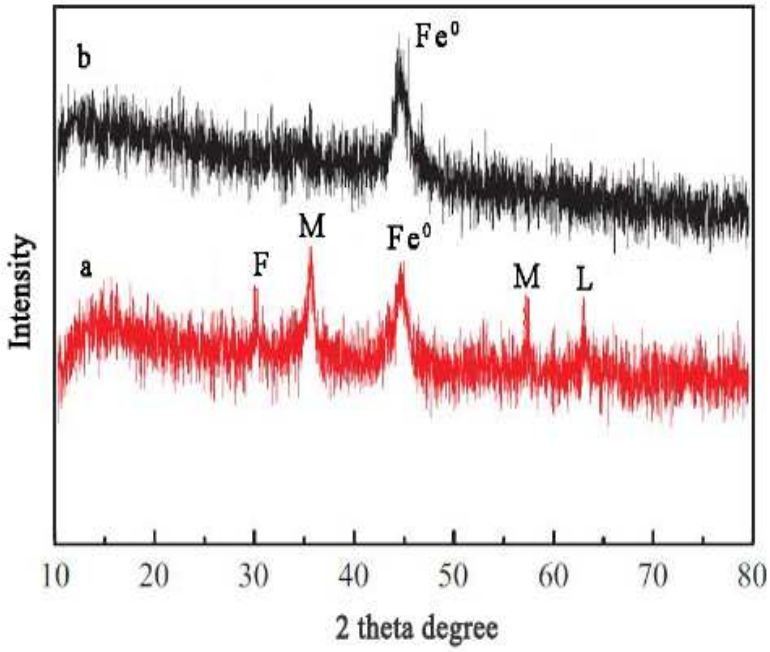

Fig. 4 - XRD patterns of samples. a. NZVI; b. 0.1 wt% SNZVI. F = ferrous oxide, M = magnetite/maghemite, L = lepidocrocite.

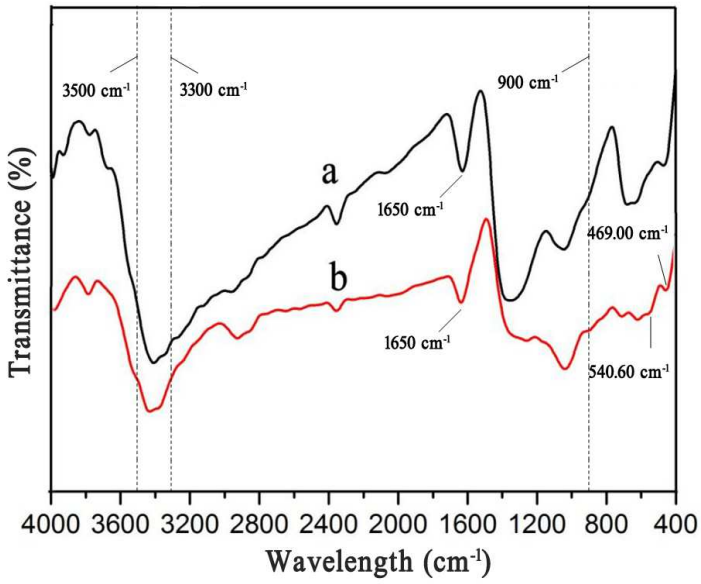

Fig. 5 - FTIR spectra of sample. a. NZVI; b. 0.1 wt% SNZVI.

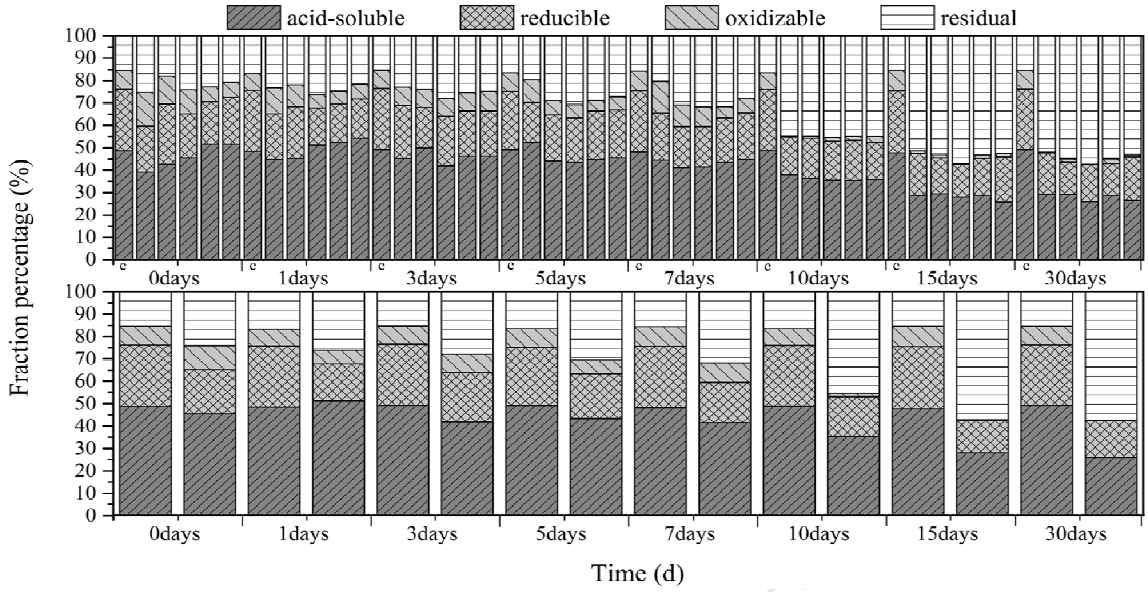

Fig. 6 - Fractioning of Cd in sediment with the addition of SNZVI (0, 0.05, 0.1, 0.15, 0.2 wt%) and varied as the incubation proceeded. (Concentration of NZVI or SNZVI: 0.5 g/L). a. SNZVI (0, 0.05, 0.1, 0.15, 0.2 wt%); b. SNZVI (0.1 wt%).

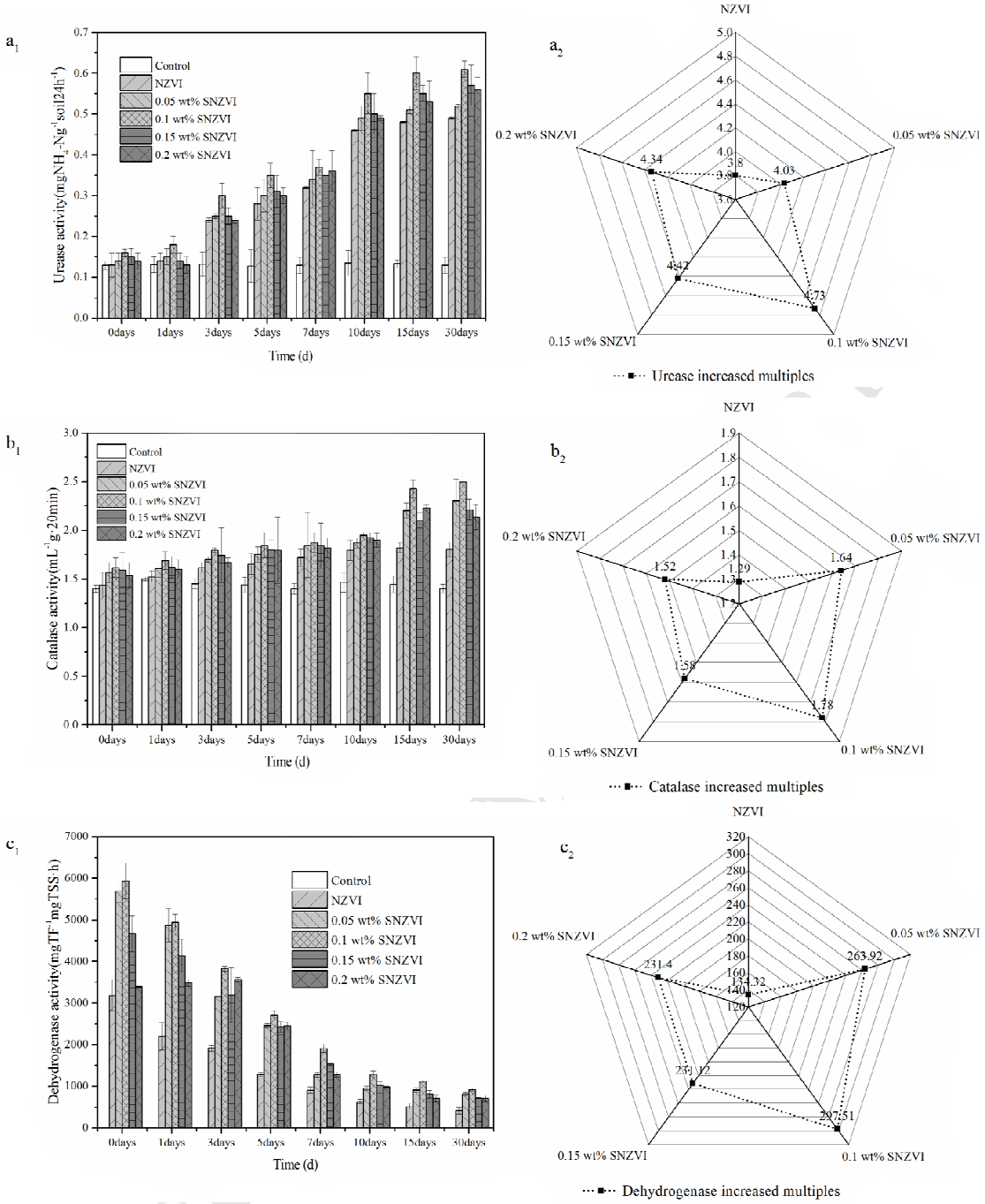

Fig. 7 - Enzyme activities under different treatments of SNZVI (0, 0.05, 0.1, 0.15, 0.2 wt%) and enzyme activities increased multiples at 30 days. a_1. Urease; a_2. Urease increased multiples (0.1 wt% SNZVI); b_1. Catalase; b_2. Catalase increased multiples (0.1 wt% SNZVI); c_1. Dehydrogenase; c_2. Dehydrogenase increased multiples (0.1 wt% SNZVI). Error bars indicate standard deviation (n = 3).

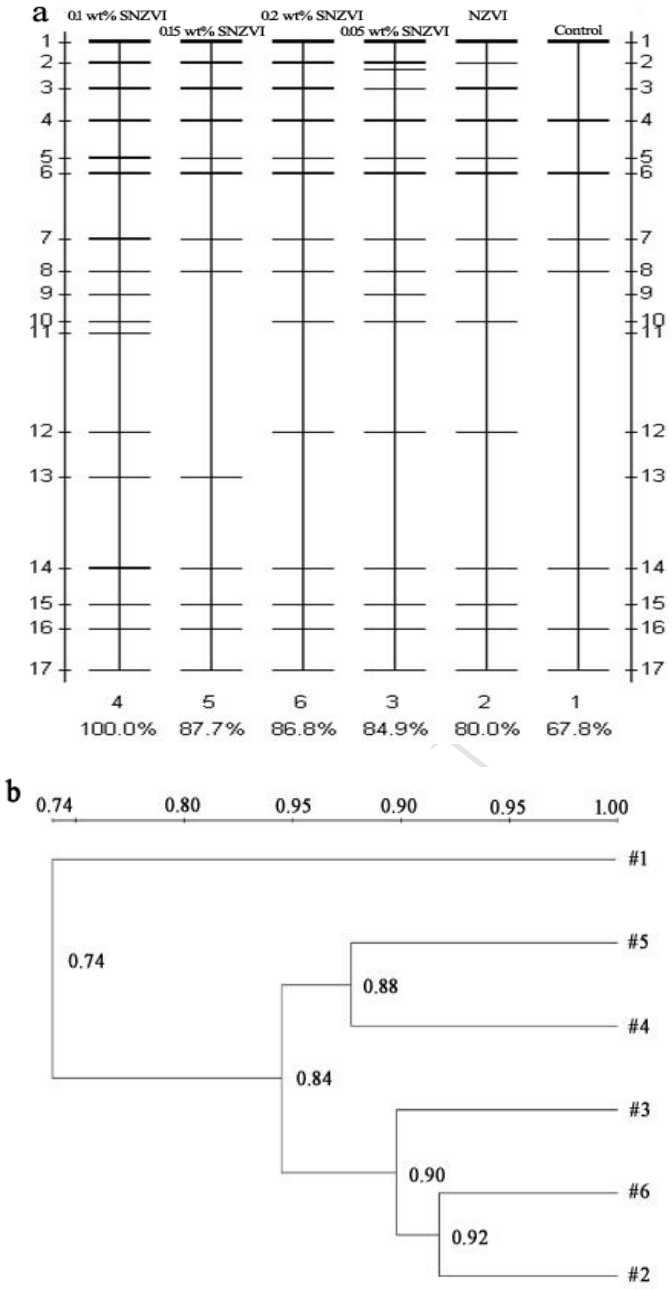

Fig. 8 - Similarity dendrograms and cluster analysis of banding patterns generated by PCR-DGGE of 16S rRNA fragments from SNZVI (0, 0.05, 0.1, 0.15, 0.2 wt%) treated samples. a. similarity dendrograms; b. cluster analysis.

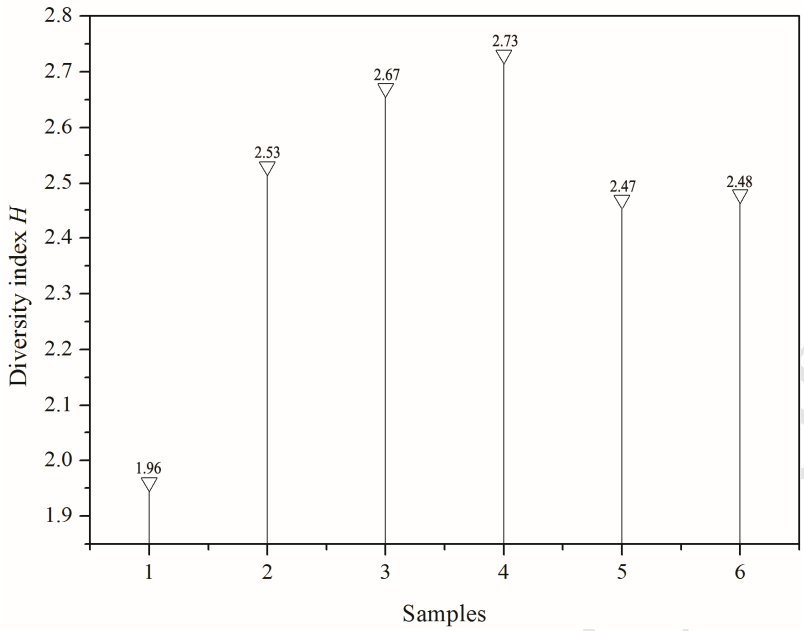

Fig. 9 - The diversity index H rooted in DGGE profiles of amplified bacterial 16S rRNA genes. The sample (2, 3, 4, 5, 6) represents the different concentrations of SNZVI (0, 0.05, 0.1, 0.15, 0.2 wt%), the sample 1 as control group.

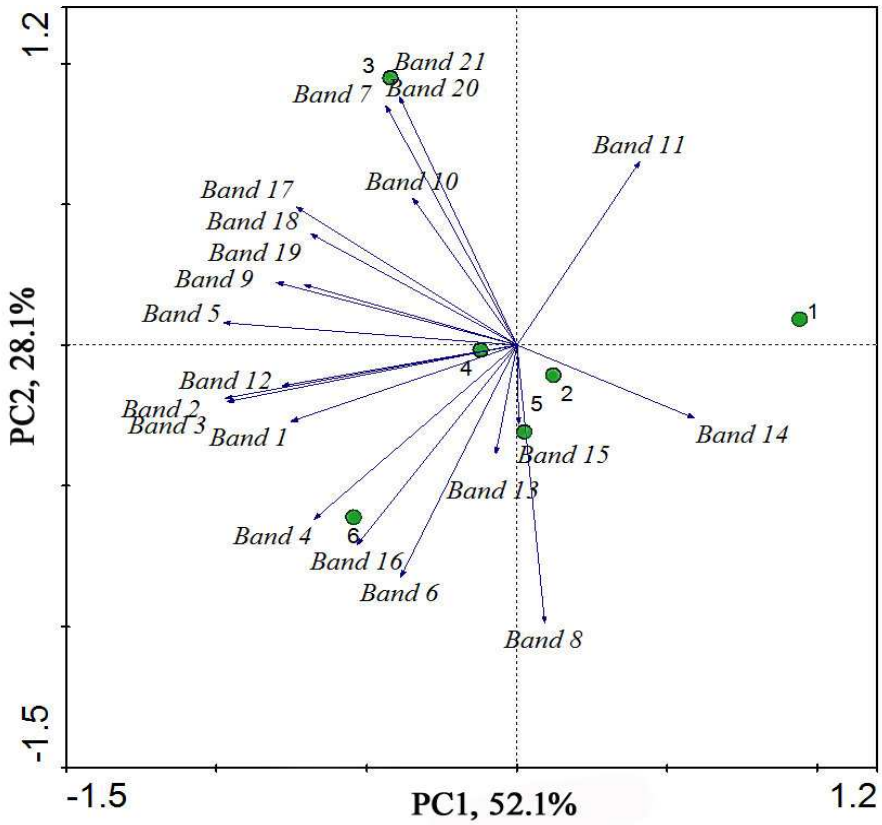

Fig. 10 - Loading plot. Eigenvectors calculated by PCA using the response variables i) relative abundance of microbial population and ii) different samples: SNZVI (0, 0.05, 0.1, 0.15, 0.2 wt%) and control group. Color circular represented 6 samples taken from two systems. The angles between arrows indicate correlations between two variables.

Highlights

- SNZVI applied to the remediation of Cd contaminated river sediments can affect Cd mobility.
- We investigated the relativity between Cd mobility and changes in enzyme activities as well as bacterial community diversity.
- The maximum residual percentage of Cd increases from 15.49% to 57.28% after 30 days of incubation at 0.1 wt% SA.
- SNZVI and NZVI could increase bacterial taxa and improve bacterial abundance.